Ion Acceleration By Single Pass Ion Cyclotron Heating In The VASIMR Engine

IEPC-2005-093

Edgar A. Bering, III[*] and Michael Brukardt[†]

University of Houston, Houston, TX, 77204-5005, USA

Franklin R. Chang-Díaz[‡], Jared P. Squire[§], Timothy W. Glover[**], Verlin Jacobson[††], Alfonso Tarditi[‡‡], and Greg McKaskill[§§]

AdAstra Rocket Company, Houston, TX, 77058, USA

and

Roger D. Bengtson[***]

University of Texas at Austin, Austin, TX 78712

   The Variable Specific Impulse Magnetoplasma Rocket (VASIMR) is a high power magnetoplasma rocket, capable of Isp/thrust modulation at constant power. The plasma is produced by helicon discharge. The bulk of the energy is added by ion cyclotron resonance heating (ICRH.) Axial momentum is obtained by adiabatic expansion of the plasma in a magnetic nozzle. Thrust/specific impulse ratio control in the VASIMR is primarily achieved by the partitioning of the RF power to the helicon and ICRH systems, with the proper adjustment of the propellant flow. Ion dynamics in the exhaust were studied using probes, gridded energy analyzers (RPA's), microwave interferometry and optical techniques. This paper will review 3 years of single-pass ICRH ion acceleration data. During this interval, the available power to the helicon ionization stage has increased from 3 to 20 kW.   The increased plasma density has produced increased plasma loading of the ICRH antenna and isignificant improvements in antenna coupling efficiency and in ion heating efficiency.

Nomenclature

η_A	=	ICRH antenna efficiency
η_b	=	ion coupling efficiency
f	=	frequency
f_{ci}	=	ion cyclotron frequency

[*] Professor, Physics and Electrical and Computer Engineering, eabering@uh.edu.
[†] Research Assistant, Physics, korjik56@hotmail.com.
[‡] President and CEO, ASPL, franklin@adastratechnologies.com .
[§] Senior Research Scientist, ASPL, jared.squire@adastratechnologies.com.
[**] Research Scientist, ASPL, tim.glover@adastratechnologies.com.
[††] Research Engineer, ASPL, verlin.jacobson@adastratechnologies.com.
[‡‡] Senior Research Scientist, ASPL, alfonso.tarditi@adastratechnologies.com.
[§§] Research Engineer, ASPL, greg.mac@adastratechnologies.com.
[***] Professor, Physics, bengtson@physics.utexas.edu.

|		
F	=	ion velocity phase space distribution function
Γ_i	=	total ion flux
I_{sp}	=	specific impulse
L_A	=	inductance of the ICRH antenna
L_M	=	inductance of the ICRH antenna matching network
m_{doti}	=	mass flow rate
P_{plasma}	=	ICRH RF power broadcast into plasma
P_{ion}	=	ICRH RF power coupled into ions
P_{ICRH}	=	ICRH RF power into antenna
Q_c	=	quality factor of the ICRH antenna coupling circuit
R_c	=	resistance of the ICRH antenna coupling circuit
R_p	=	plasma loading of the ICRH antenna
Θ	=	pitch angle
v_{ICRF}	=	exhaust plasma flow velocity with ICRH on
$v_{helicon}$	=	exhaust plasma flow velocity with helicon only
$VSWR_{plasma}$	=	voltage standing wave ratio of the ICRH antenna, with plasma present
$VSWR_{vacuum}$	=	voltage standing wave ratio of the ICRH antenna, with no plasma present
W_{ICRH}	=	mean ion energy increase owing to ICRH
ω	=	angular frequency
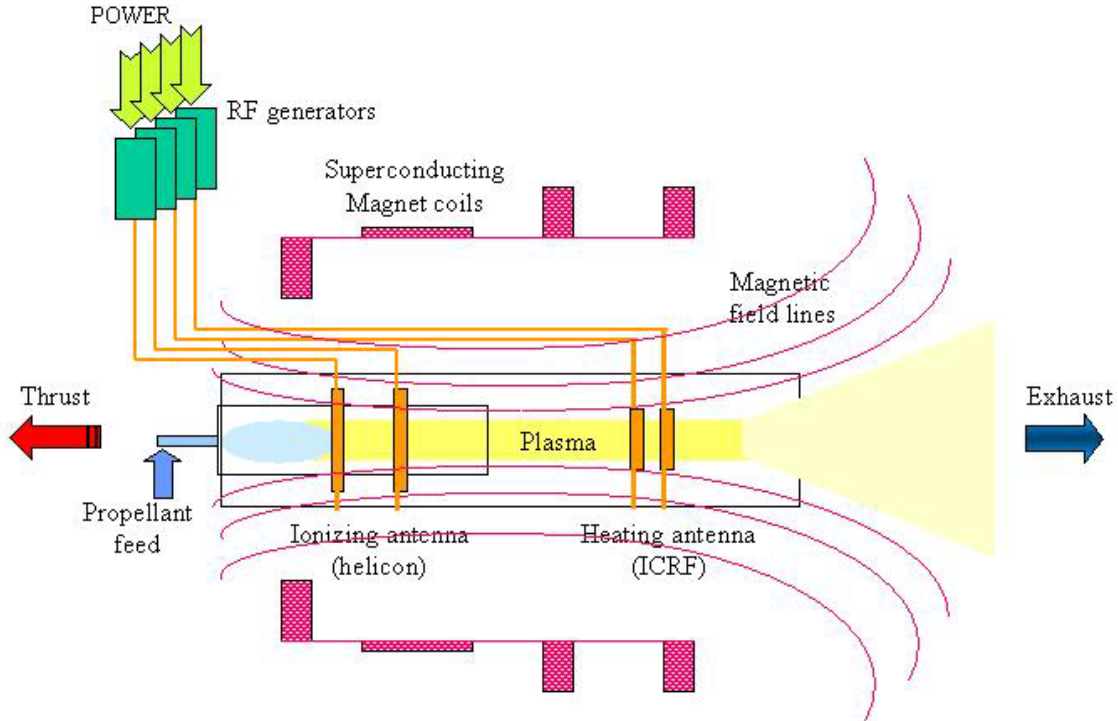
Figure 1. Cartoon block diagram of the VASIMR system, illustrating the basic physics.

I. Introduction

THE Variable Specific Impulse Magnetoplasma Rocket (VASIMR) is a high power, radio frequency-driven magnetoplasma rocket, capable of I_{sp}/thrust modulation at constant power[1-5]. The physics and engineering of this device have been under study since 1980. A simplified schematic of the engine is shown in Figure 1. The VASIMR consists of three main sections: a helicon plasma source, an ICRH plasma accelerator, and a magnetic nozzle[1, 3, 4, 6-8]. Figure 1 shows these three stages integrated with the necessary supporting systems. One key aspect of this concept is its electrode-less design, which makes it suitable for high power density and long component life

by reducing plasma erosion and other materials complications. The magnetic field ties the three stages together and, through the magnet assemblies, transmits the exhaust reaction forces that ultimately propel the ship. The plasma is produced by an integrated helicon discharge[9-12]. The bulk of the plasma energy is added in a separate downstream stage by ion cyclotron resonance heating (ICRH) [13-17]. Axial momentum is obtained by the adiabatic expansion of the plasma in a magnetic nozzle. Thrust/specific impulse ratio control in the VASIMR is primarily achieved by the selective partitioning of the RF power to the helicon and ICRH systems, with the proper adjustment of the propellant flow. However, other complementary techniques are also being considered. A NASA-led, research effort, involving several teams in the United States, continues to explore the scientific and technological foundations of this concept. The research is multifaceted and involves theory, experiment, engineering design, mission analysis, and technology development. Experimentally, high-density stable plasma discharges have been generated in Helium, Hydrogen, Deuterium, Argon and Xenon. Ion dynamics in the exhaust are studied using a variety of probes, gridded energy analyzers (RPA's), microwave interferometry and optical techniques.

The VASIMR engine has three major subsystems, the injection stage, the heating stage and the nozzle[8]. The use of a separate injection system has allowed us to optimize our system for maximum power efficiency over a wide range of gas flow rates. At present, the best choice appears to be a helicon discharge[9-12]. The next stage downstream is the heating system. Energy is fed to the system in the form of a circularly polarized RF signal tuned to the ion cyclotron frequency. ICRH heating has been chosen because it transfers energy directly and solely to the ions, which maximizes the efficiency of the engine[14, 15]. The system also features a two-stage magnetic nozzle, which accelerates the plasma particles by converting their rotational energy into directed momentum. The detachment of the plume from the field takes place mainly by the loss of adiabaticity and the rapid increase of the local plasma β, defined as the local ratio of the plasma pressure to the magnetic pressure.

An important consideration involves the rapid absorption of ion cyclotron waves by the high-speed plasma flow. This process differs from the familiar ion cyclotron resonance utilized in tokamak fusion plasma as the particles in VASIMR pass under the antenna only once[3, 18-20]. Sufficient ion cyclotron wave (ICW) absorption has nevertheless been predicted by recent theoretical studies[21]. The light ion VASIMR engine is best suited to high power operation. The critical factor that limits efficiency at low power is amount of antenna loading that can be obtained with the ICRH system. The load impedance of the antenna must be significantly larger than the impedance of the transmission and matching network. The cyclotron resonance frequency of deuterium in the available magnetic field is about 2 MHz, which means that one requires plasma that is ~8-10 centimeters in diameter before reasonable load impedances are obtained. It takes a high power system to produce such plasma. The successful demonstration of single pass ICRH acceleration of light ion plasma in the VX-10 machine was reported last year[3,4,22].

Elimination of a magnetic bottle from the VASIMR concept was motivated by theoretical modeling of single-pass absorption of the ion cyclotron wave on a magnetic field gradient by theorists at the University of Texas at Austin[21]. While the cyclotron heating process in the confined plasma of fusion experiments results in approximately thermalized ion energy distributions, the non-linear absorption of energy in the single-pass process produces a boost, or displacement of the ion kinetic energy distribution. The ions are immediately ejected through the magnetic nozzle before the ion distribution has had time to thermalize. Hence, VASIMR is not an electrothermal rocket, and the fusion term "ICRH" for ion cyclotron resonant heating may be misleading in describing the process now used in VASIMR, if the term "heating" implies a thermalized distribution. "ICRA", with the "A" standing for absorption or perhaps acceleration, is more accurate if we are referring to the non-linear, non-thermal absorption process modeled by UT-Austin and exhibited by natural processes in the auroral region. For example, single-pass ICRH ion acceleration has been invoked to explain observations of "ion conic" energetic ion pitch angle distributions in the auroral regions of the Earth's ionosphere and magnetosphere[23-29]. The fact that ion conics are commonly found on auroral field lines suggests that ICRH is a ubiquitous process in auroral arcs. The efficiency of the wave-particle coupling that single pass heating can produce is illustrated by the fact that space-borne observations of ion-cyclotron waves are relatively rare[30-38].

The subject of this paper is to present the data from a series of experiments that have conclusively demonstrated single pass ICRH in fast-flowing laboratory plasma. This paper will focus on the retarding potential analyzer (RPA) data in order to describe the improvements made during the past year and highlight some of the experimental results that have been obtained. We explored the details of the ion dynamics in deuterium exhaust plasma using ~19 kW of RF power to the helicon ionization stage and 1.3 kW to the ICRH acceleration stage. Owing to significant reductions in ionization cost, the total ion flux in the exhaust plasma is an order of magnitude greater than the flux obtained during the experiments that were reported as recently as November of last year. In this high-density plasma, the available energy per ion is reduced compared to last year, but the booster efficiency of the ICRH process has increased. Ion energization of ~17 eV/ion has been demonstrated in this higher-flux plasma. This energy increase

corresponds to booster efficiency (η_b) of 85%, in agreement with model predictions. Results also confirm conversion of transverse ion motion to axial motion via conservation of the first adiabatic invariant.
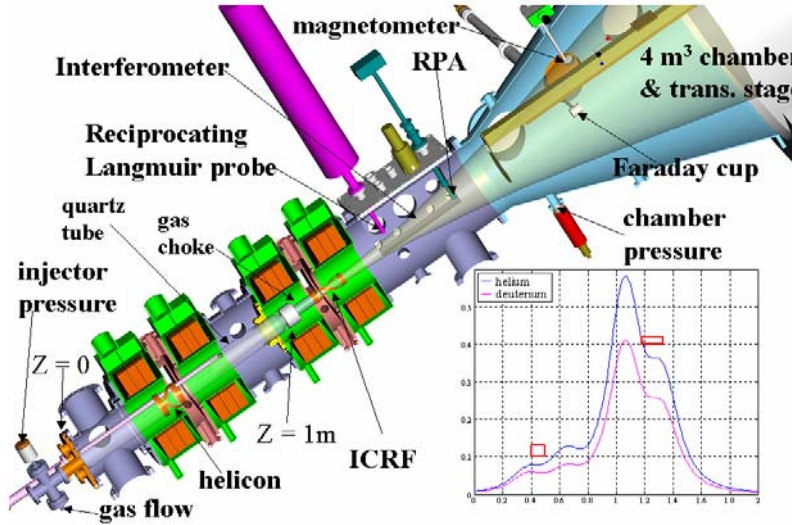
II.   Experiment

Figure 2. Engineering drawing of the VX-25, showing the major systems and the location of the diagnostic instruments.

The VASIMR engine has three major subsystems, the injection stage, the heating stage and the nozzle[8]. A laboratory simulation of a 4.5-30 kW physics demonstrator VASIMR engine has been under development and test at NASA-JSC for several years[39, 40]. The details of the engine and its design principles have been previously reported[3, 41]. A more specific detailed view of the present physics demonstrator laboratory experiment (VX-25) is shown in Figure 2. The use of a separate injection system has allowed us to optimize our system for maximum power efficiency over a wide range of gas flow rates. At present, the best choice appears to be a helicon discharge[9-12]. The next stage downstream is the heating system. Energy is fed to the system in the form of a circularly polarized rf signal tuned to the ion cyclotron frequency. ICRH heating has been chosen because it transfers energy directly and largely to the ions, which maximizes the efficiency of the engine[14, 15]. In the present small-scale test version, there is no mirror chamber and the ions make one pass through the ICRH antenna. The system also features a two-stage magnetic nozzle, which accelerates the plasma particles by converting their azimuthal energy into directed momentum. The detachment of the plume from the field takes place mainly by the loss of adiabaticity and the rapid increase of the local plasma β, defined as the local ratio of the plasma pressure to the magnetic pressure.

The main VASIMR vacuum chamber is a cylinder 1.8 m long and 35.6 cm in diameter. The VASIMR exhaust flows through a conical adapter section into a 5-m^3 exhaust reservoir. The magnetic field is generated by four liquid nitrogen cooled 150 turn copper magnets, which can generate a magnetic induction of up to 1.5 T. The high vacuum pumping system consists of a cryopump and two diffusion pumps with a combined total capacity of 5000 l/s.

In recent years, a NASA-led, multifaceted research effort, involving several teams in the United States, continues to explore the scientific and technological foundations of this concept, and its extrapolation as a high power, in-space propulsion system[8, 41]. Experimentally, two major facilities are investigating plasma performance. Both have obtained attractive results with deuterium and helium, the two propellants of choice. In both gasses, densities of 10^{20} m^{33} have been obtained at frequencies ~4 times the lower hybrid resonance. Slightly lower densities, in range of 10^{18} m^{-3} have been obtained with hydrogen.

Over the course of the investigations reported here, there have been a series of improvements and upgrades to the helicon plasma source[42, 43]. The earliest experiments that will be presented were performed using a 5 cm diameter "Boswell" type double saddle antenna and 3 kW of rf power. Directionality was provided by use of a magnetic cusp configuration. Over the 2.5-year interval spanned by the experiments reported here, the helicon has undergone a number of successive upgrades. The helicon plasma source in the VASIMR engine has been incrementally improved in three steps. First, antenna size, connector and power supply improvements raised the available power from 3 kW to 10 kW, still operating with Boswell antenna and a magnetic cusp. The factors limiting the application of rf power to the helicon ionizing discharge had been the power of the 25 MHz transmitter (3 kW), the voltage limits on the vacuum rf feed-through, the voltage limits of the rf matching network and the diameter of the discharge. Successive steps to 9 cm increased the diameter of the helicon antenna. The helicon rf supply was completely rebuilt. A new high voltage power supply was built, along with a new high power transmitter. A 10 kV rf vacuum feed-through was

obtained and installed, along with a new high voltage matching network. These new components produced helium plasma operating at 10 kW, with ~4 times the ion flux achievable at 3 kW. Second, the transmitting antenna was changed from the Boswell configuration to a helical half-twist antenna. Finally, the decision was taken to switch transmitters and power the helicon with our 100 kW transmitter, which can operate the helicon at 13.5 MHz up to 24 kW before connector and cable voltage limits are reached.

The ICRH antenna uses a helical, double strap quarter-turn configuration developed by our colleagues at Oak Ridge National Laboratory. It is polarized to launch left-handed slow mode waves[19, 44]. The present configuration of the rf booster or ICRH system uses 1.5 kW of 1.5-2.5 MHz left hand polarized slow mode waves launched from the high field, over dense side of the resonance (region 13 of the Clemmow-Mullaly-Allis (CMA) diagram, using the *Stix*[17] notation. The antenna is uncooled and connected via a low-voltage feedthrough, which limits power to 1.5 kW.

A. Diagnostics

Available plasma diagnostics include a triple probe, a Mach probe, a bolometer, a television monitor, an H-a photometer, a spectrometer, neutral

Figure 3. A sample shot of RPA data, showing relationship of chamber ground to plasma potential.

gas pressure and flow measurements, several gridded energy analyzers (retarding potential analyzer or RPA)[4,8,45-49], a surface recombination probe system, an emission probe, a directional, steerable RPA and other diagnostics[50]. The Langmuir[51] probe measures electron density and temperature profiles and the Mach[52-54] probe measures flow profiles. Together this gives total plasma particle flux. An array of thermocouples provides a temperature map of the system. The Langmuir probe has four molybdenum tips that are biased as a triple probe, with an extra tip for measuring electrostatic fluctuations[51]. The Mach probe has two molybdenum tips biased in ion saturation, one upstream and one downstream of a stainless steel separator.

1. Retarding Potential Analyzer (RPA)

Retarding potential analyzer (RPA) diagnostics have been installed to measure the accelerated ions. The present RPA is a planar ion trap located ~40 cm downstream from the plane of the triple and Mach probes, which corresponds to a factor of 8 reduction in the magnetic field strength. The grids are 125-wire/in nickel mesh, spaced 1 mm apart with Macor spacers. The opening aperture is 1 cm in diameter, nominally centered on the plasma beam. A four-grid configuration is used, with entrance attenuator, electron suppressor, ion analyzer and secondary suppressor grids.
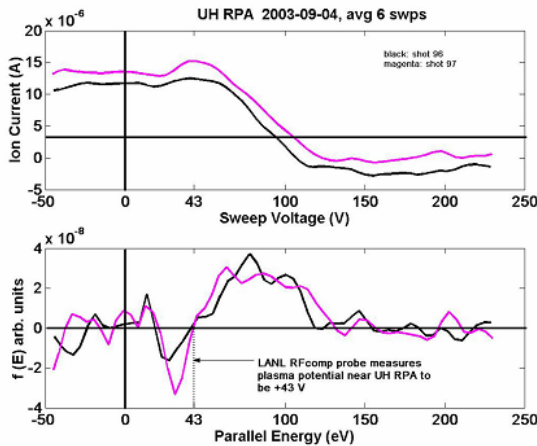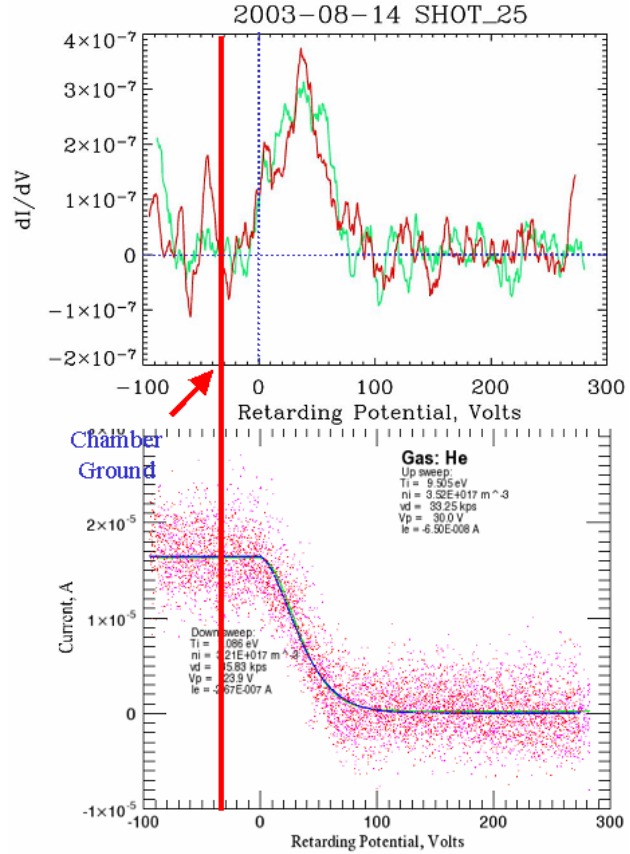
Figure 4. Two sample shots of RPA data, with 0 V set to chamber ground, showing the relationship between plasma potential as measured by an rf compensated Langmuir probe and the sweep potential where $dI/dV \approx 0$. The LANL RF compensated probe gives $V_p \approx 45$ V. This value was used for analysis of summer 2003 data. The direct LANL/RPA comparison shots always put V_p at the $dI/dV \approx 0$ point.

The interpretation of RPA output data in terms of ion energy requires an accurate knowledge of plasma potential (V_p). On University of Houston (UH) RPA plots, the 0 of the retarding potential scale is set to V_p as shown in Figure 3, instead of chamber ground. Thus, the sweep scale can be read directly as ion energy in eV. When available, data from an rf compensated swept Langmuir probe provided by Los Alamos National Laboratory (LANL) are used to determine V_p, as

Figure 5. Circuit diagram of the ICRH antenna, indicating how the plasma impedance couples to the circuit.

shown in Figure 4 (*M. Light*, personal communication, 2003). When other V_p data are not available, plasma potential is assumed to be the value at which *dI/dV* first significantly exceeds 0, which usually agrees with the LANL probe value within the error bars. This value is typically ~+30-50 V with respect to chamber ground. The operator biases the body and entrance aperture of the RPA to this value. The solid lines on the raw data plots are the results of least squares fits of drifting Maxwellians to the up and down sweeps[45,46,49,55].

We can find an upper limit to rf smearing of the current-voltage characteristic of the RPA by examining T_i estimates from Maxwellian fits to the data from the coldest plasma shots obtained. The coldest ion temperature observed with ICRH off was 0.7 eV observed with a very high gas flow. The coldest ion temperature during an ICRH on shot was ~1 eV. These temperatures represent experimental upper limits on the rf contamination of ion temperature estimates.
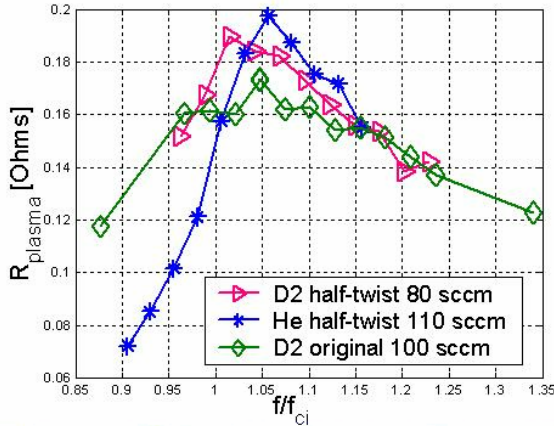

Figure 6. Plasma loading as a function of ICRH frequency for a deuterium plasma produced by a 3 kW helicon discharge.
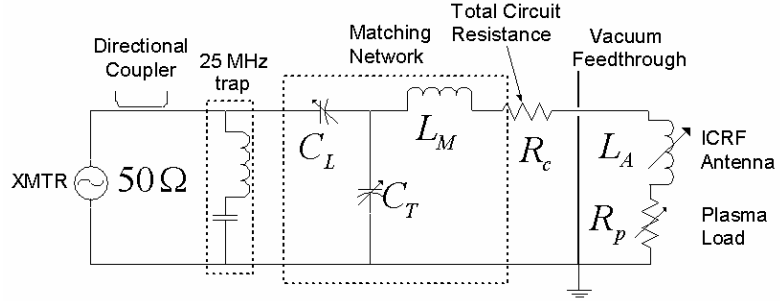
III. Data

A. Plasma Loading

The light ion VASIMR engine is best suited to high power operation. The critical factor that limits efficiency at low power is the efficiency of helicon stage and hence the ionization cost[56]. At high power, the ICRH stage is more important and hence ICRH antenna loading is more critical here. The load impedance of the antenna must be significantly larger than the impedance of the transmission and matching network (see Figure 5). The cyclotron resonance frequency of helium in the available magnetic field is about 2 MHz, which means that one requires plasma that is ~8-10 centimeters in diameter before reasonable load impedances are obtained.

The following calculation illustrates how plasma loading is determined. Using the relationship that:

$$\frac{VSWR_{plasma}}{VSWR_{vacuum}} = \frac{(R_p + R_c)}{R_c}, \tag{1}$$

a network analyzer is used in place of the high power rf transmitter to measure the quality factor of the antenna coupling circuit and to tune the circuit when no plasma is present. Then we have:

$$R_c = \frac{\omega(L_M + L_A)}{Q_c} \approx 0.24\Omega \tag{2}$$

and

$$R_p = R_c(VSWR_{plasma} - 1). \tag{3}$$

Thus the coupling efficiency is:

$$\eta_A = \frac{R_p}{(R_p + R_c)} = 0.89 \tag{4}$$

The power radiated into the plasma is estimated as:

$$P_{plasma} = \eta_A P_{ICRH} = 1.25\text{kW} \tag{5}$$

The initial deuterium loading data were taken when only 4 kW of helicon power was available. Plasma loading was generally maximum when $f/f_{ci} > 1$, as shown in Figure 6. As shown in this figure, the plasma loading was comparable to the circuit resistance. Helium data showed similar behavior.

More recent loading measurements have been made using a 20 kW helicon discharge. The measurements in Figure 7 show very good loading, ~2 Ω, which implies a corresponding high coupling efficiency, as shown in Figure 8. This high loading impedance was obtained with a sizable, ~ 1 cm plasma-antenna gap. Maximum in the loading occurred at $f/f_{ci} = 0.95$, indicating that the antenna was launching a more propagating wave than it was in the low density case.

B. Low Density Plasma

The earliest convincing results were obtained with a 3 kW helicon discharge using a ``Boswell'' type helicon antenna during the summer of 2003[3, 4, 42-44]. The effect of the ICRH heating is expected to be an increase in the component of the ion velocity perpendicular to the magnetic field. This increase will take place in the resonance region, i.e. the location where the injected rf wave frequency is equal to the ion cyclotron frequency. Downstream of the resonance, this perpendicular heating will be converted into axial flow owing to the requirement that the first adiabatic invariant of the particle motion be conserved as the magnetic field decreases. Since the total ion flux is not expected to increase, this axial acceleration should be accompanied by a density decrease.
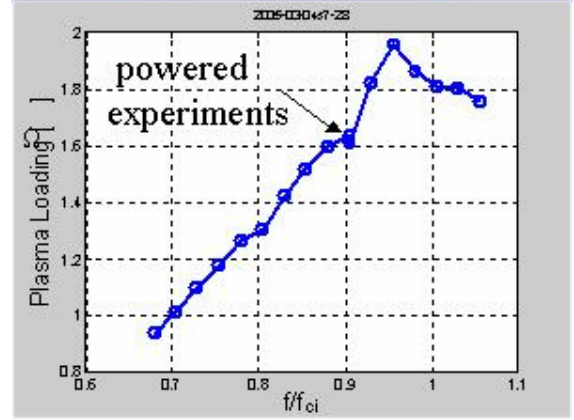

Figure 8. Plasma loading as a function of ICRH frequency for a high density deuterium plasma produced by a 20 kW helicon discharge.
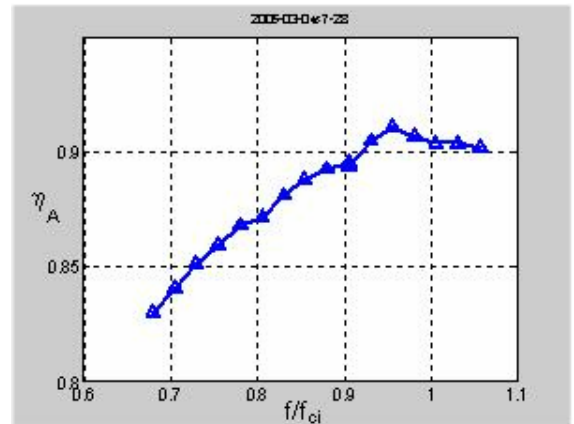

Figure 8. Antenna efficiency corresponding to the data in Fig. 7.

7

Furthermore, the particles should have a pitch angle distribution that does not peak at 0º Instead, the distribution should peak at an angle that maps to a perpendicular pitch angle at resonance. Therefore a collimated detector oriented along the magnetic field should observe a decrease in total flux and an increase in particle energy. As the acceptance angle of the detector is increased, the ion saturation current should start to show an increase when the acceptance cone includes the peak in the pitch angle distribution. Low-density data from 2003 have been reported previously and will not be discussed here.

C. Higher Density Plasma
1. 8.3 kW helicon discharge

Since March, 2004, the primary efforts of the VASIMR team have concentrated on improving ionization efficiency. This focus on the helicon has meant that the density and total ion flux of the plasma available to be heated has steadily increased without a corresponding increase in ICRH power. Figure 9 shows the effect of applying 1.3 kW to deuterium plasma produced by the Boswell antenna operating at 8.3 kW. The gas input rate was 100 sccm. The figure shows a time series of plasma parameters obtained from least squares fitting a single drifting Maxwellian to each separate RPA sweep obtained during one shot. The shot sequence was initiated at 2009:45.0 UT. ICRH was turned on at 45.9s. The data show that the application of ICRH doubled the plasma flow speed. The observed speed corresponds to an I_{sp} ~ 9000 s.

The fundamental dynamical quantity is the ion velocity phase space distribution function, F. The distribution functions for both the ICRH-on and ICRH-off conditions shown in Figure 9 are plotted in Figure 10, measured at 0º pitch angle. This figure shows that in the case of deuterium, charge exchange losses between the ICRH antenna and the RPA do not obscure the effect of ICRH, in contrast to the case of helium. In Figure 10, it is clear that the entire plasma has been accelerated, with very little left behind.

A bi-Maxwellian model representation has been used to fit the data taken during a scan of the location of the ICRH resonance region with respect to the antenna[57-60]. Increasing the current to the mirror field magnet, which increases the magnetic induction at the mirror thus moving the resonance downstream, performs this scan. Moving the resonance away
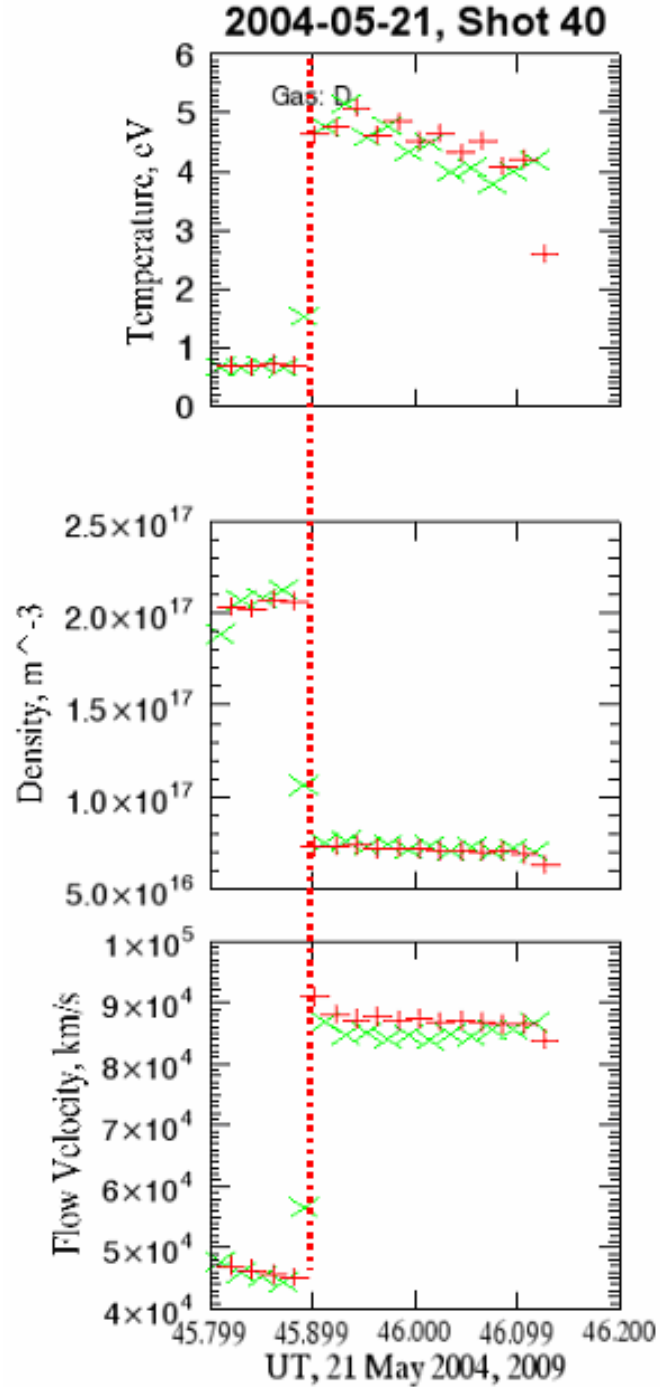

Figure 9. Fit parameters obtained by least squares fitting a drifting Maxwellian representation to each voltage sweep obtained by the wide angle RPA during a pulsed ICRH helium plasma shot. From top to bottom, the panels show ion drift velocity, ion density and ion temperature in the frame of the beam. The plusses and X's show up and down sweeps. The vertical dashed line show the time when the ICRH turned on.
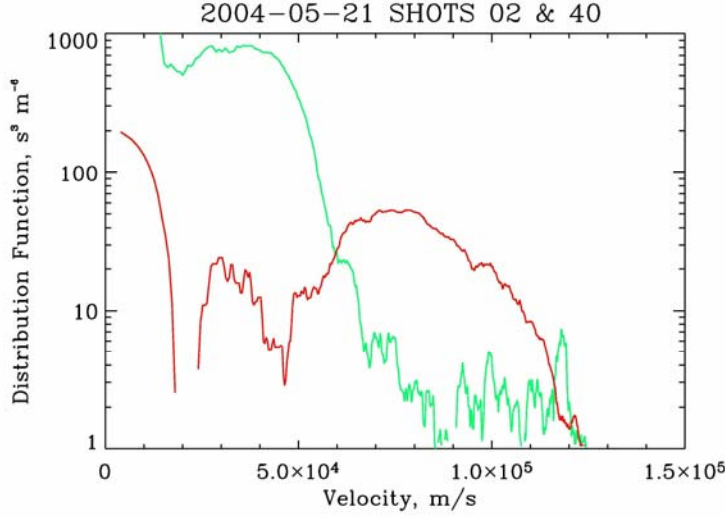
Figure 10. The ion velocity phase space distribution functions obtained during both the ICRH-on portion of the deuterium shot shown in Figure 11 and an ICRH-off shot run under otherwise identical conditions. The ICRH off curve is shown as a lighter- -colored (green) line.

from the antenna significantly reduces the plasma loading of the antenna, which means that less rf power is being fed to the plasma. The results of this experiment, interpreted using the bi-Maxwellian approach, are shown in Figure 12. There are several points to be made concerning the results shown in Figure 12. The best loading and coupling is achieved when the resonance is located under the antenna. The velocity of the "slow" component is still in excess of 70 km/s near optimum. The density of the faster component exceeds the slow component density, and the estimated output power increase corresponds to or exceeds model estimates for the antenna configuration at that time. These models predicted an ion coupling efficiency of 40-50% at this plasma density.

The next example of an ICRH experiment that will be presented is a radial scan of the RPA during both ICRH ion and off conditions. The results have been interpreted using a single Maxwellian and are shown in Figure 11. This experiment was performed with a 10 kW helical antenna discharge. Under these conditions, the plasma loading of the ICRH antenna had been increased from ~0.2 Ω to ~2 Ω, resulting in an increase in antenna efficiency to ~0.89.

These results can be integrated to estimate the output power and momentum flux in the exhaust plume. Using the ion flow rate determined by the triple probe, which has a more accurate absolute calibration than the RPA, the power balance corresponds well to model predictions. The measured power input to the ion flux was found to have been

$$P_i = \tfrac{1}{2}\dot{m}_i\left(v_{ICRH}^2 - v_{helicon}^2\right) = 430 \text{ to } 591 \text{ W.} \tag{6}$$

Given a coupling efficiency at the time when Figs. 10 and 11 were obtained of

$$\eta_B = \frac{P_i}{P_{plasma}} = 36 \text{ to } 49\%, \tag{7}$$

the momentum flux output of the device during these particular runs was estimated to have been:

$$\dot{m}_i v_{ICRH} = 14 \text{ to } 19 \text{ mN} \tag{8}$$

$$\dot{m}_i v_{helicon} = 7 \text{ to } 10 \text{ mN} \tag{9}$$

The momentum flux inferred from the RPA and triple probe data agrees with the results of a direct momentum flux measurement with a mechanical probe in that the momentum flux with ICRH-on is observed to double. The absolute value of the momentum flux inferred from the RPA and probe measurements is hard to compare directly with the momentum flux probe owing to the fact that the flux probe paddle does not intercept the entire plasma.
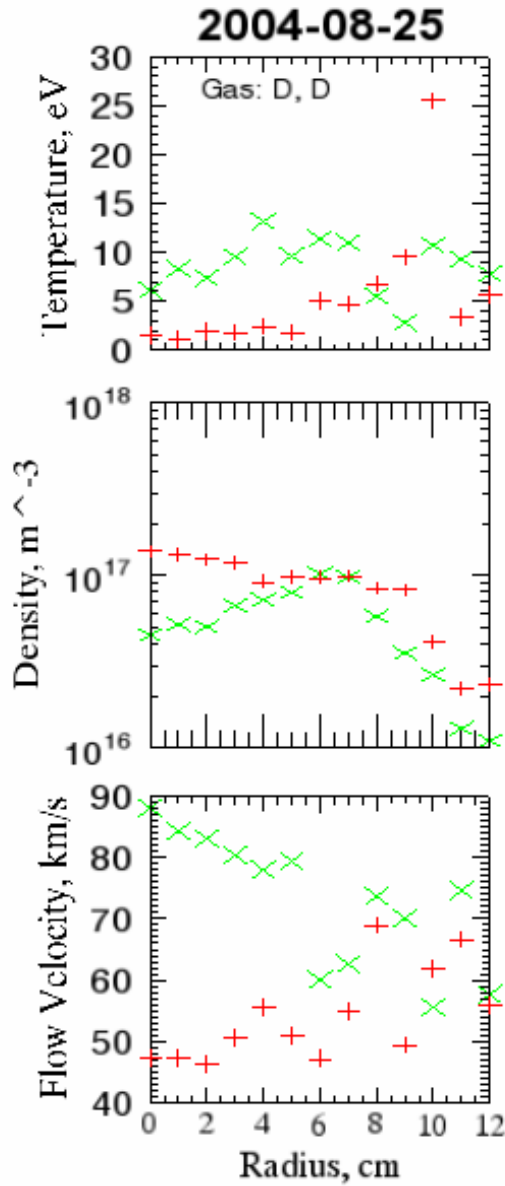
2004-08-25

2004-05-21

Figure 11. Fit parameters obtained by least squares fitting drifting Maxwellian representations to RPA data taken while scanning the radial location of the RPA during both ICRH-on (X's) and ICRH-off (+'s) conditions. Each symbol represents the average of all sweeps during a single shot.
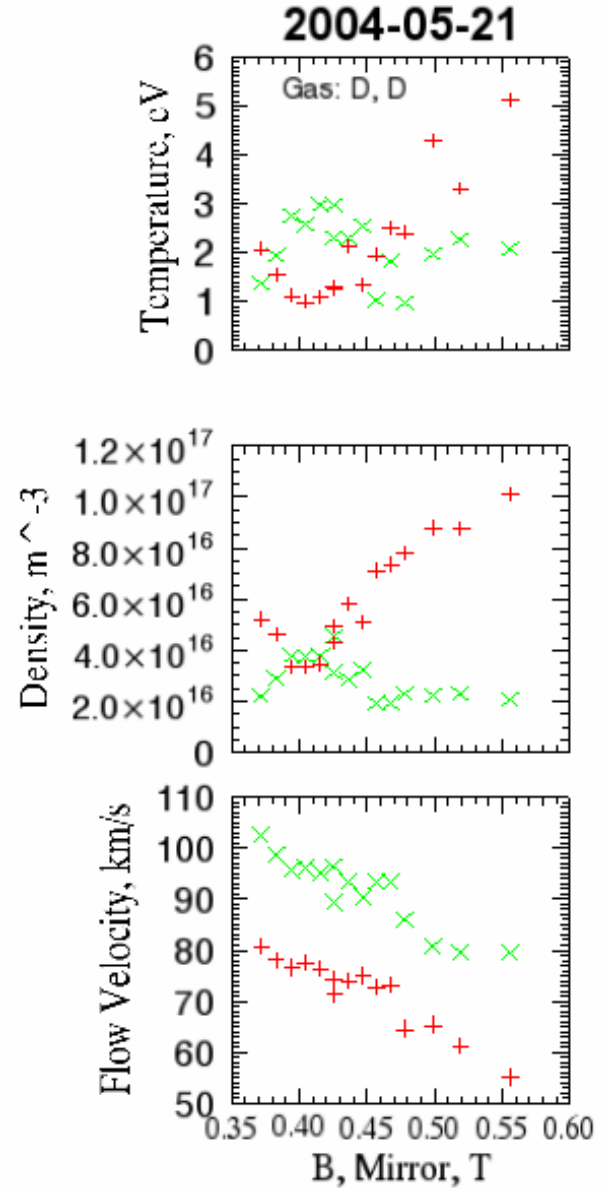
Figure 12. it parameters obtained by least squares fitting drifting bi-Maxwellian representations to the RPA data obtained during a scan of mirror magnet field intensity. From top to bottom, the panels show ion drift velocity, ion density and ion temperature in the frame of the beam. The plusses show the slow, hot component. The X's show the fast, cold accelerated component.

2. 20 kW helicon discharge

The most recent improvements in the helicon discharge have both increased the available power to 20 kW and reduced the energy cost per ion to ~200eV per ion pair. These improvements have combined to give nearly an order of magnitude increase in total ion flux. On the other hand, because of the emphasis on helicon improvements, available ICRH power has stayed constant at 1.5 kW. Conservation of energy considerations require that we should observe a substantial reduction in the energy increase per ion obtained with constant power ICRH provided the

The 29ᵗʰ International Electric Propulsion Conference, Princeton University,
October 31 – November 4, 2005

damping is not so severe as to prevent ICRH wave power from penetrating the entire plasma column. Figure 13 compares the ion energy distributions detected by the RPA in a 20 kW deuterium discharge showing the effect of the ICRH. The figure shows clear evidence of ion acceleration by a mere 1.5 kW of ICRH. The observed energy increase was 17 eV/ion, yielding plasma with more than twice the bulk kinetic energy obtainable with the helicon alone

Full ion velocity phase space distribution functions can be obtained by rotating the RPA, shot-to-shot[61, 62]. Two dimensional color contour plots of a planar cut through the distribution function are shown in Figure 14 for ICRH-off and Figure 15 for ICRH-on. Since a pitch angle of 90° at the location of the maximum field intensity maps to a pitch angle of 10° at the location of the RPA, all of the ions in
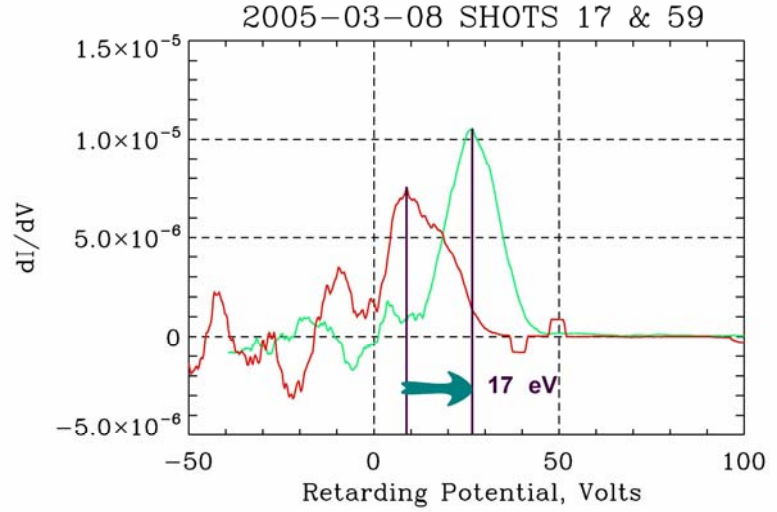

Figure 13. The first derivative of the current-voltage characteristics measured by an RPA with 30° collimation. The lower, lighter curve shows a deuterium shot without ICRH, and the upper, darker curve shows a deuterium shot with ICRH.

both distributions that have pitch angles Θ>10° have been scattered, presumably by an ion-neutral collisions. There is a clear, visible difference between the two distributions, indicating that the ICRH has accelerated the entire plasma. The reduction in the maximum value of the distribution function in the ICRH on case corresponds to a 0.55 density drop. This decrease is consistent with the results of simultaneous interferometer observations.

The total ion flux during these shots was measured using a number of independent methods, including interferometers, reciprocating triple probe and an array of small planar Langmuir probes. The radial density profiles determined by the array of small Langmuir probes for both ICRH-on and ICRH-off conditions comparable to those shown in Figs. 13-15 are shown in Figure 16. The plasma flux was measured well downstream (~0.7 m) of the ICRH antenna. The figure shows that the profile narrowed when ICRH was applied. However, the integrated flux does not change substantially with the application of ICRH.

A total ion flux was obtained:

$$\Gamma_i = 3.1 \pm 0.6 \times 10^{20} \text{ s}^{-1} \tag{10}$$

As noted above, the RPA data indicate that the ICRH gave the ions a mean energy increase of:

$$W_{ICRH} = 17 \pm 2 \text{ eV} \tag{11}$$

The product of these two numbers gives the total power increase in the exhaust plume, as follows:

$$P_{ion} = \Gamma_i W_{ICRH} = 840 \pm 190 \text{ W} \tag{12}$$

The ICRH power that has been radiated into the plasma may be estimated using the antenna efficiency, η_A=89%, that was determined from the plasma loading measurements:
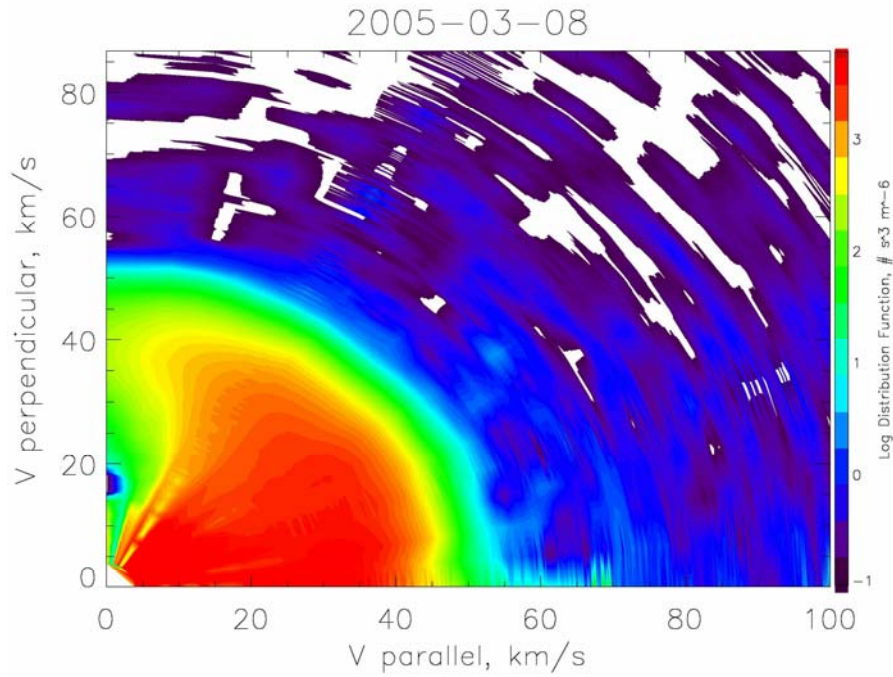
Figure 15. The ion velocity phase space distribution function obtained in a 20 kW deuterium discharge with no ICRH. The color bar scale is logarithmic.
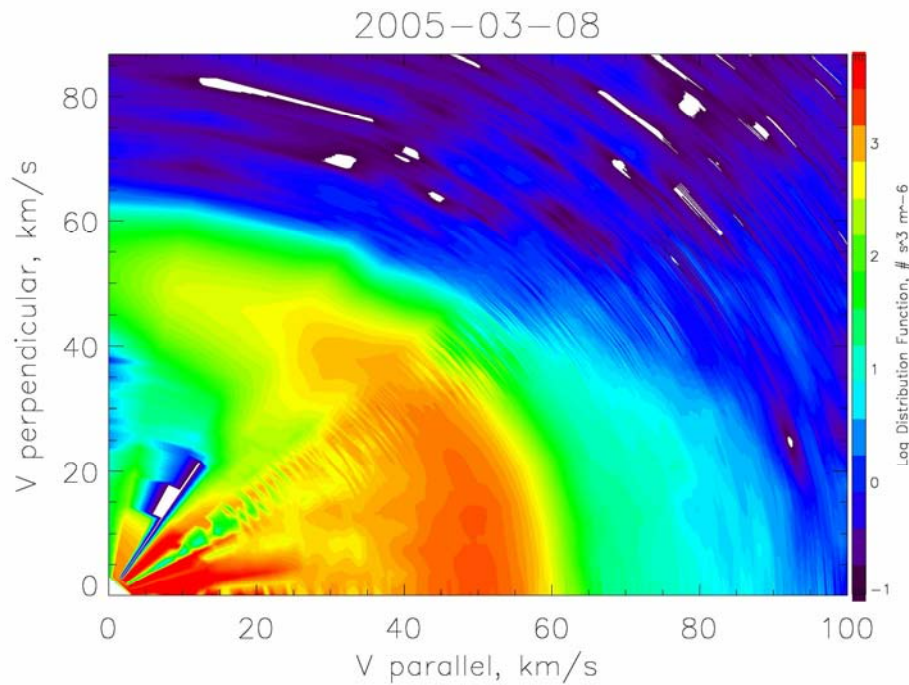

Figure 14. The ion velocity phase space distribution function obtained in a 20 kW deuterium discharge with 1.5 kW of ICRH on. The color bar scale is logarithmic.

$$P_{plasma} = \eta_A P_{ICRH} = 1.25 \text{ kW} \tag{13}$$

Finally, we obtain an estimate of the efficiency of the ICRH process, as follows:

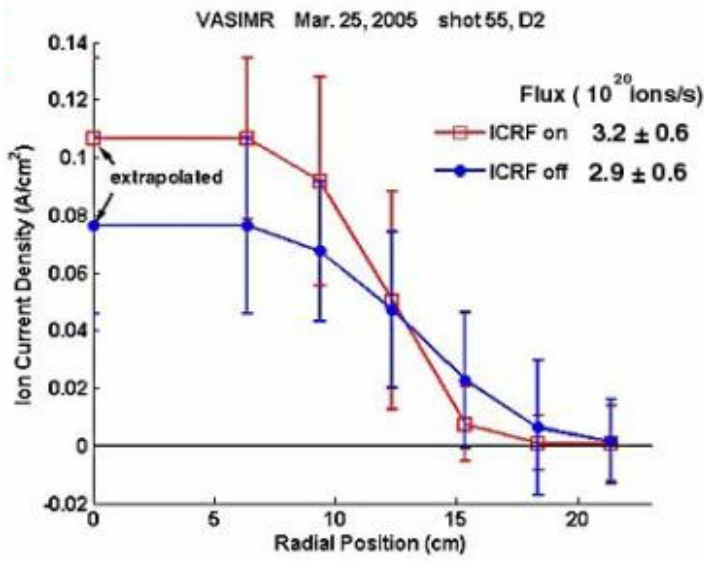$$\eta_{ICRH} = \frac{P_{ion}}{P_{plasma}} = 67 \pm 15\% \tag{14}$$

Figure 16. Ion density plotted as a function of radial position during high density discharges similar to those shown in Figs. 13-15. Density was measured by an array of ~ 1 cm diameter planar Langmuir probes. Profiles for both ICRH-off and ICRH-on are compared.

Absorption efficiency of this order is high enough to suggest the possibility that the ion cyclotron wave was fully damped prior to reaching the center of the plasma column. This situation was investigated by means of another RPA radial scan (Figure 17). Figure 17 indeed shows a drop in bulk flow velocity and corresponding increase in ion density in the innermost 1 cm of the plasma column. This hole would indicate that 1.5 kW is insufficient signal strength to fully illuminate the discharge that the experiment presently produces. Since the data in Figs. 13 and 15 were taken at the center of the column, it is likely that the ion energization, power deposited and ICRH efficiency estimates just presented are systematically low.

IV. Conclusions

Substantial progress has been made in the development of the VASIMR engine. In the past two years, the operating power level of the helicon discharge has been increased by nearly an order of magnitude, to 20-24 kW. The energy cost per ion pair has been reduced to ~200-250 eV. Plasma loading of the ICRH antenna increases with increasing total ion flux and plasma density. Using present maximum helicon discharge output, loading impedance in excess of 2 Ω is being obtained, which corresponds to $\eta_A > 90\%$. The challenges for the coming year are to raise the ICRH power level to 20 kW and to improve the directionality and modal purity of the ICRH antenna to the point where $\eta_B > 80\%$.
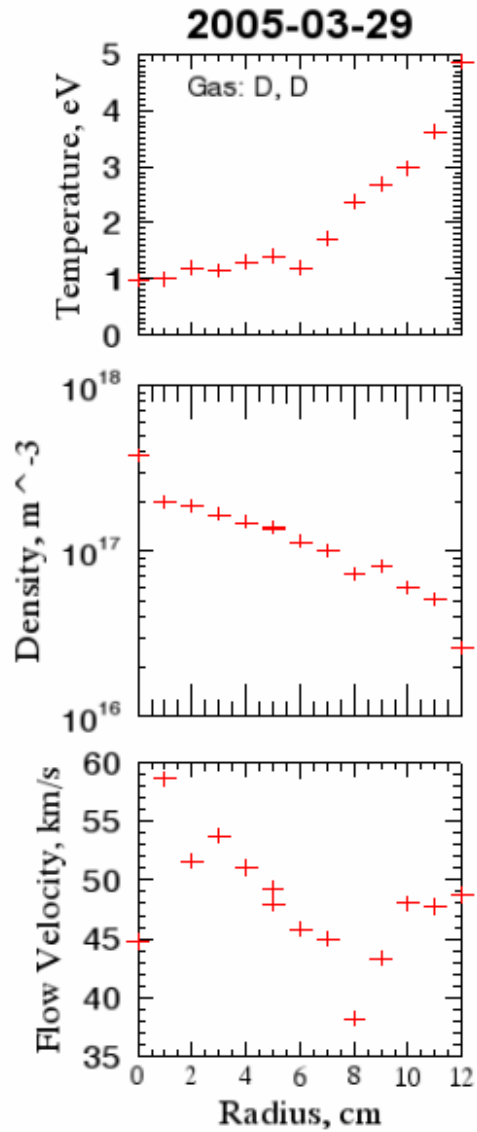
.

Figure 17. Fit parameters obtained by least squares fitting drifting Maxwellian representations to RPA data taken while scanning the radial location of the RPA during ICRH-on (X's) conditions during high density discharges similar to those shown in Figs. 13-15. Each symbol represents the average of all sweeps during a single shot.

References

[1]F. R. Chang Díaz, "Research status of the Variable Specific Impulse Magnetoplasma Rocket," presented at the 39th Annual Meeting of the Division of Plasma Physics, 1997 (unpublished).

[2]F. R. Chang Díaz, "The VASIMR Engine," Scientific American 283 (5), 72-79 (2000).

[3]F. R. Chang Díaz, J. P. Squire, T. Glover et al., "The VASIMR Engine: Project Status and Recent Accomplishments," presented at the 42nd Aerospace Sciences Meeting and Exhibit, Reno, NV, 2004.

[4]E. A. Bering III, F. R. Chang Díaz, J. P. Squire et al., "Velocity phase space studies of ion dynamics in the VASIMR engine," presented at the 42nd AIAA Aerospace Sciences Meeting and Exhibit, Reno, NV, 2004.

[5]E. A. Bering III, F. R. Chang-Díaz, and J. P. Squire, "The use of RF waves in space propulsion systems," Bulletin of Radio Science (310), 92-106 (2004).

[6]F. R. Chang Díaz, "Research Status of the Variable Specific Impulse Magnetoplasma Rocket," presented at the Open Systems, July 27-31, 1998, Novosibirsk, Russia, 1998 (unpublished).

[7]F. R. Chang Díaz, J. P. Squire, A. V. Ilin et al., "Development of the VASIMR Engine, The," presented at the International Conference of Electromagnetics in Advanced Space Applications, Sep 13-17, 1999, Torino, Italy, 1999 (unpublished).

[8]F. R. Chang Díaz, J. P. Squire, E. A. Bering III et al., "VASIMR Engine Approach to Solar System Exploration, The," presented at the 39th AIAA Aerospace Sciences Meeting and Exhibit, Jan. 8-11, 2001, Reno, NV, 2001.

[9]R. W. Boswell, "Very efficient plasma generation by whistler waves near the lower hybrid frequency," Plasma Phys. Control. Fusion 26, 1147 (1984).

[10]F. F. Chen, "Plasma ionization by helicon waves," Plasma Physics and Controlled Fusion 33 (4), 339-364 (1991).

[11]R. W. Boswell and F. F. Chen, "Helicons - The Early Years," IEEE Transactions on Plasma Science 25 (6), 1229-1244 (1997).

[12]R. W. Boswell and C. Charles, "The helicon double layer thruster," presented at the 28th International Electric Propulsion Conference, IEPC 2003, Toulouse, France, 2003.

[13]N. J. Fisch, "Confining a tokamak plasma with rf-driven currents," Physical Review Letters 41 (13), 873 (1978).

[14]S. N. Golovato, K. Brau, J. Casey et al., "Plasma Production and Heating in a tandem mirror central cell by radio frequency waves in the ion cyclotron frequency range," Phys. Fluids 31 (12), 3744-3753 (1988).

[15]Y. Yasaka, R. Majeski, J. Browning et al., "ICRF heating with mode control provided by a rotating field antenna," Nuclear Fusion 28, 1765 (1988).

[16]D.G. Swanson, *Plasma Waves* (Academic Press, Boston, 1989).

[17]T. H. Stix, *Waves in Plasma* (American Institute of Physics, New York, NY, 1992).

[18]E. A. Bering III, M. Brukardt, F. R. Chang-Díaz et al., "Experimental studies of the exhaust plasma of the VASIMR engine," presented at the 40th AIAA Aerospace Sciences Meeting and Exhibit,, Reno, NV, 2002.

[19]E. A. Bering III, M. S. Brukardt, W. A. Rodriguez et al., "Ion Dynamics and ICRH Heating in the Exhaust Plasma of The VASIMR Engine," presented at the 53rd International Astronautical Congress / The World Space Congress, 10-19 Oct 2002, Houston, Texas, 2002 .

[20]D. G. Chavers and F. R. Chang-Díaz, "Momentum flux measuring instrument for neutral and charged

particle flows," Rev. Sci. Instrum. 73 (10), 3500-3507 (2002).

[21]B. N. Breizman and A. V. Arefiev, "Single-Pass Ion Cyclotron Resonance Absorption," Physics of Plasmas 8 (3), 907-915 (2001).

[22]E. A. Bering III, F. R. Chang-D\'íaz, J. P. Squire et al., "Ion velocity phase space studies of the VASIMR engine exhaust plasma,," presented at the 46th Annual Meeting of the Division of Plasma Physics, APS, Savannah, GA, 2004 (unpublished).

[23]E. G. Shelley, R. D. Sharp, and R. G. Johnson, "Satellite observations of an ion acceleration mechanism," Geophysical Research Letters 3 (11), 654 (1976).

[24]R. D. Sharp, R. G. Johnson, and E. G. Shelley, "Observation of an ionospheric acceleration mechanism producing energetic (keV) ions primarily normal to the geomagnetic field direction," Journal of Geophysical Research 82, 3324 (1977).

[25]F. S. Mozer, C. W. Carlson, M. K. Hudson et al., "Observations of paired electrostatic shocks in the polar shocks in the polar magnetosphere," Physical Review Letters 38, 292 (1977).

[26]A. G. Ghielmetti, R. G. Johnson, R. D. Sharp et al., "The latitudinal, diurnal and altitudinal distributions of upward flowing energetic ions of ionospheric origin," Geophysical Research Letters 5, 59 (1978).

[27]E. G. Shelley, "Heavy ions in the magnetosphere," Space Science Reviews 23, 465 (1979).

[28]R. D. Sharp, R. G. Johnson, and E. G. Shelley, "Energetic particle measurements from within ionospheric structures responsible for auroral acceleration processes," Journal of Geophysical Research 84, 480 (1979).

[29]H. L. Collin, R. D. Sharp, E. G. Shelley et al., "Some general characteristics of upflowing ion beams over the auroral zone and their relationship to auroral electrons," Journal of Geophysical Research 86, 6820 (1981).

[30]E. A. Bering III, M. C. Kelley, and F. S. Mozer, "Observations of an intense field aligned thermal ion flow and associated intense narrow band electric field oscillations," Journal of Geophysical Research 80 (34), 4612-4620 (1975).

[31]E. A. Bering III and M. C. Kelley, "Observation of Electrostatic Ion Cyclotron Waves at the Boundary of an Auroral Arc," EOS, Transactions, American Geophysical Union 56, 173 (1975).

[32]M. C. Kelley, E. A. Bering III, and F. S. Mozer, "Evidence that the electrostatic ion cyclotron instability is saturated by ion heating," Physics of Fluids 18, 1590-1597 (1975).

[33]P. M. Kintner, M. C. Kelley, and F. S. Mozer, "Electrostatic hydrogen cyclotron waves near one earth radius altitude in the polar magnetosphere," Geophysical Research Letters 5, 139 (1978).

[34]P. M. Kintner, M. C. Kelley, R. D. Sharp et al., "Simultaneous observations of energetic (keV) upstreaming ions and electrostatic hydrogen cyclotron waves," Journal of Geophysical Research 84, 7201-7212 (1979).

[35]P. M. Kintner, "On the distinction between electrostatic ion cyclotron waves and ion cyclotron harmonic waves," Geophysical Research Letters 7, 585 (1980).

[36]P. M. Kintner, W. Scales, J. Vago et al., "Harmonic H^+ gyrofequency structures in auroral hiss observed by high-altitude auroral sounding rockets," Journal of Geophysical Research 96 (A6), 9627-9638 (1991).

[37]E. A. Bering III, "Apparent Electrostatic Ion Cyclotron Waves in the Diffuse Aurora," Geophysical Research Letters 10, 647-650 (1983).

[38]E. A. Bering III, "The Plasma Wave Environment of an Auroral Arc, 1., Electrostatic Ion Cyclotron Waves in the Diffuse Aurora," Journal of Geophysical Research 89, 1635-1649 (1984).

[39]J. P. Squire, F. R. Chang-Díaz, V. T. Jacobson et al., "Helicon plasma injector and ion cyclotron acceleration development in the VASIMR experiment," presented at the 36th AIAA/ASME/SAE/ASEE Joint Propulsion Conference, July17-19, 2000, Huntsville, Alabama, 2000.

[40]A. Petro, F. R. Chang-Díaz, A. V. Ilin et al., "Development of a space station-based flight experiment for the VASIMR magneto-plasma rocket," presented at the 40th AIAA Aerospace Sciences Meeting and Exhibit, 14-17 January 2002, Reno, NV, 2002.

[41]F. R. Chang Díaz, "An overview of the VASIMR engine: High power space propulsion with RF plasma generation and heating," presented at the 14th Topical Conference on Radio Frequency Power in Plasmas, May 7-9, 2001, Oxnard, CA, 2001.

[42]T. W. Glover, F. R. Chang-Díaz, V. T. Jacobson et al., "Ion Cyclotron Heating Results in the VASIMR VX-10," presented at the 40th AIAA/ASME/SAE/ASEE Joint Propulsion Conference and Exhibit, Fort Lauderdale, FL, 2004.

[43]E. A. Bering III, J. P. Squire, G. McCaskill et al., "Progress Toward the Development of a 50 kW VASIMR Engine," presented at the 43rd AIAA Aerospace Sciences Meeting and Exhibit, Reno, NV, 2005.

[44]F. R. Chang Díaz, J. P. Squire, A. V. Ilin et al., "Early Results of ICRH Experiments in VX-10," Bulletin of the American Physical Society DPP03, RP1.138 (2003).

[45]V. I. Krassovsky, "Exploration of the upper atmosphere with the help of the third Soviet sputnik," Proc. IRE 47, 289 (1959).

[46]E. C. Whipple, "The ion trap-results in "Exploration of the upper atmosphere with the help of the third SOviet sputnik"," Proc. IRE 47, 2023 (1959).

[47]L. W. Parker and E. C. Whipple, "Theory of spacecraft sheath structure, potential, and velocity effects on ion measurements by traps and mass spectrometers," Journal of Geophysical Research 75, 4720-4733 (1970).

[48]W. B. Hanson, R. A. Heelis, R. A. Power et al., "The retarding potential analyzer for Dynamics Explorer-B," Space Science Instruments 5, 503-510 (1981).

[49]S. Minami and Y. Takeya, "Ion temperature determination in the ionosphere by retarding potential analyzer aboard sounding rocket," Journal of Geophysical Research 87, 713 (1982).

[50]J. P. Squire, F. R. Chang-Díaz, R. Bengtson et al., "A plasma diagnostic set for the study of a variable specific impulse magnetoplasma rocket," presented at the APS Division of Plasma Physics Meeting, Pittsburg, PA, 1997 (unpublished).

[51]S.-L. Chen and T Sekiguchi, "Instantaneous Direct-Display System of Plasma Parameters by Means of Triple Probe," Journal of Applied Physics 36, 2363 (1965).

[52]E. A. Bering III, M. C. Kelley, F. S. Mozer et al., "Theory and operation of the split Langmuir probe," Planetary and Space Science 21, 1983-2001 (1973).

[53]P.C. Stangeby, "Measuring Plasma Drift Velocities in Tokamak Edge Plasmas Using Probes," Physics of Fluids 27 (11), 2699-2704 (1984).

[54]I.H. Hutchinson, "Ion collection by probes in strong magnetic fields with plasma flow," Physical Review A 37 (11), 4358-4366 (1988).

[55]I. H. Hutchinson, *Principles of Plasma Diagnostics* (Cambridge University Press, Cambridge, 1987).

[56]M. D. Carter, F. W. Jr. Baity, G. C. Barber et al., "Comparing Experiments with Modeling for Light Ion Helicon Plasma Sources," Physics of Plasmas 9 (12), 5097-5110 (2002).

[57]W. B. Hanson and D. D. McKibbin, "An ion-trap measurement of the ion-concentration profile above the F_2 peak," Journal of Geophysical Research 66, 1667 (1961).

[58]W. B. Hanson, S. Sanatani, D. Zuccaro et al., "Plasma measurements with the retarding potential analyzer on OGO 6," Journal of Geophysical Research 75 (28), 5483-5501 (1970).

[59]R. E. Bourdeau, E. C. Whipple, J. L. Donley et al., "Experimental evidence for the presence of helium ions based on Explorer VIII satellite data," Journal of Geophysical Research 67, 467-475 (1962).

[60]R. E. Bourdeau and J. L. Donley, "Explorer VIII satellite measurements n the upper ionosphere," Proceedings of the Royal Society A. 281, 487-503 (1964).

[61]R. L. Stenzel, R. Williams, R. Aguero et al., "Novel directional ion energy analyzer," Review of Scientific Instruments 53 (7), 1027-1031 (1982).

[62]R. L. Stenzel, W. Gekelman, N. Wild et al., "Directional velocity analyzer for measuring electron distribution functions in plasma," Review of Scientific Instruments 54, 1302-1310 (1983).